Electronic Supplementary Information

Metallic Bonds and Thermal Vibration in Brass

Toshihiko Yokoyama

yokoyama@ims.ac.jp

Department of Materials Molecular Science, Institute for Molecular Science,

Myodaiji-cho, Okazaki, 444-8585, Japan

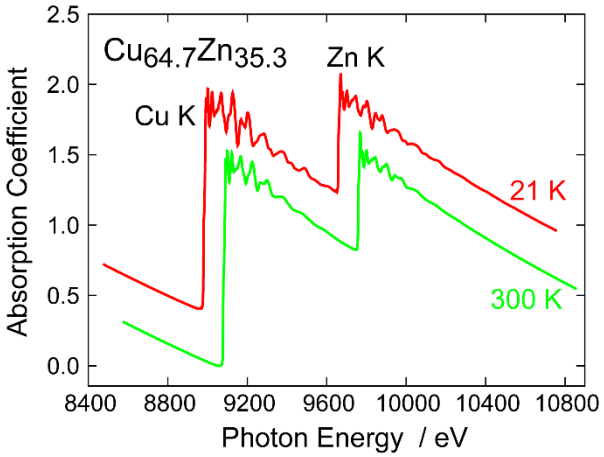

Fig. S1 Typical Cu and Zn K-edge EXAFS spectra of the brass foil at 21 and 300 K. The 300-K spectrum is shifted to the bottom right.

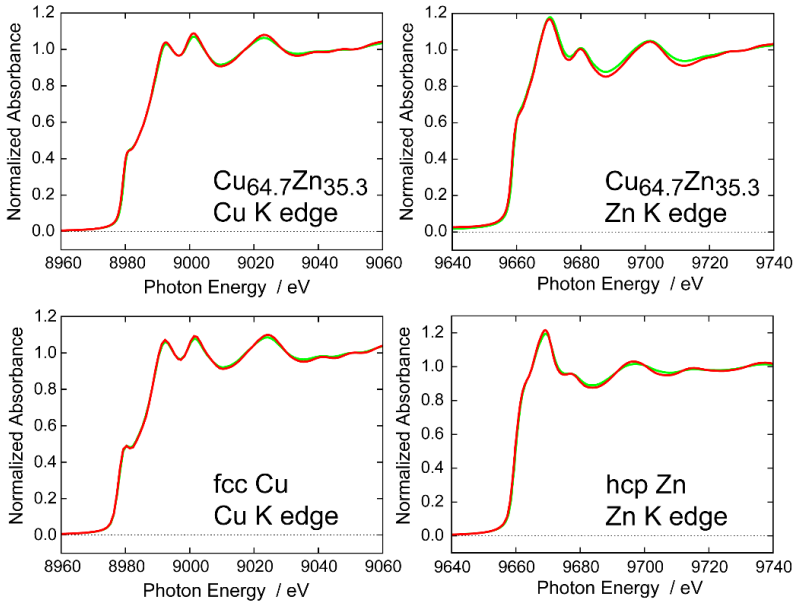

Fig. S2 Cu and Zn K-edge XANES spectra of the brass foil at 21 (red) and 300 (green) K, together with those of *fcc* Cu and *hcp* Zn foils. The Cu K-edge XANES of brass is quite similar to that of *fcc* Cu, while the Zn K-edge XANES shows a so-called white line at ~9668 eV, followed by typical *fcc* XANES features at higher photon energy. For XANES peak analysis, see the references as T. Yamamoto, *X-Ray Spectrom.* 2008, **37**, 572 and W. Olovsson, B. Alling, and M. Magnuson, *J. Phys. Chem. C*. 2016, **120**, 12890, for instance.

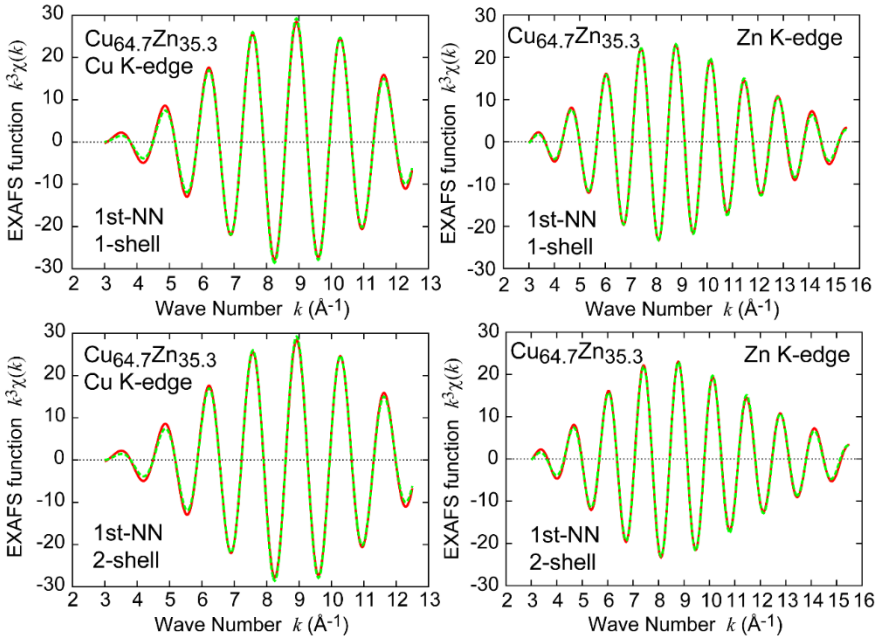

Fig. S3 Curve fitting analysis for the first-NN shells in the Cu and Zn K-edge EXAFS of the brass foil at 21 K, using the FEFF standards. As is described in the main text, the one-shell analysis is resultantly found to be more reliable.

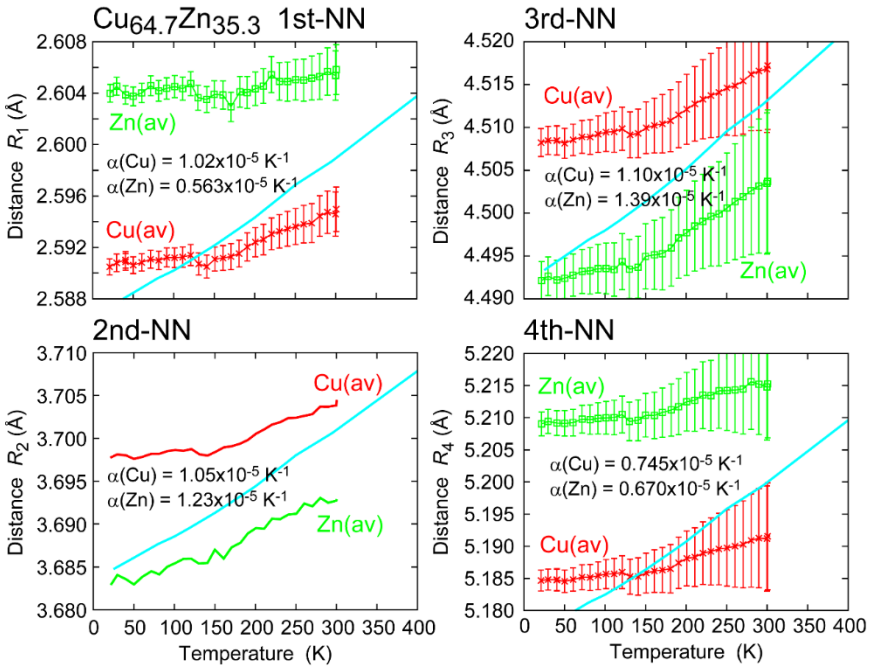

Fig. S4 Temperature dependence of the interatomic distances for the first- to fourth-NN shells in the Cu (red) and Zn (green) K-edge EXAFS of the brass foil, using the empirical standard method. The distances corresponding to the lattice constant a_0 are also depicted as a light-blue line.

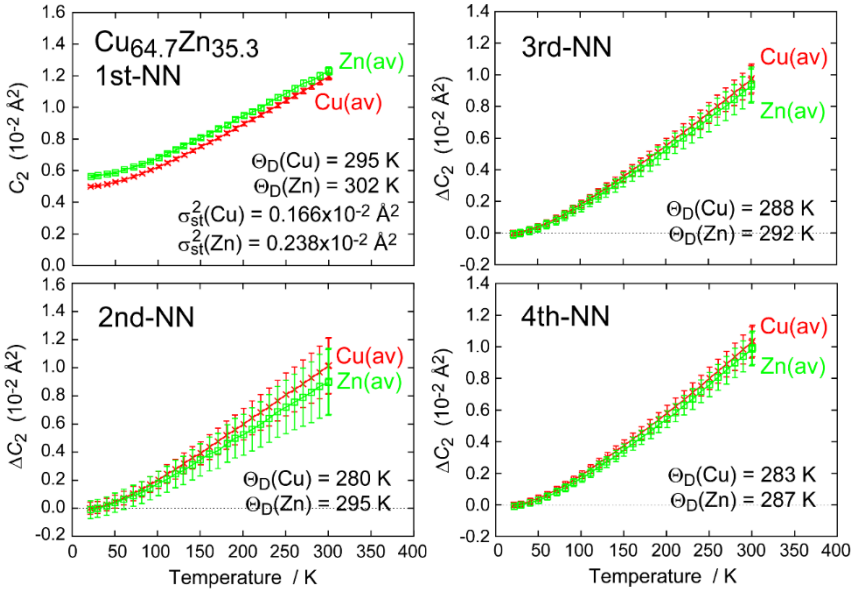

Fig. S5 Temperature dependence of the Debye-Waller factors C_2 for the first- to fourth-NN shells in the Cu (red) and Zn (green) K-edge EXAFS of the brass foil, using the empirical standard method. The estimated Debye temperature for each curve is given in the figure.

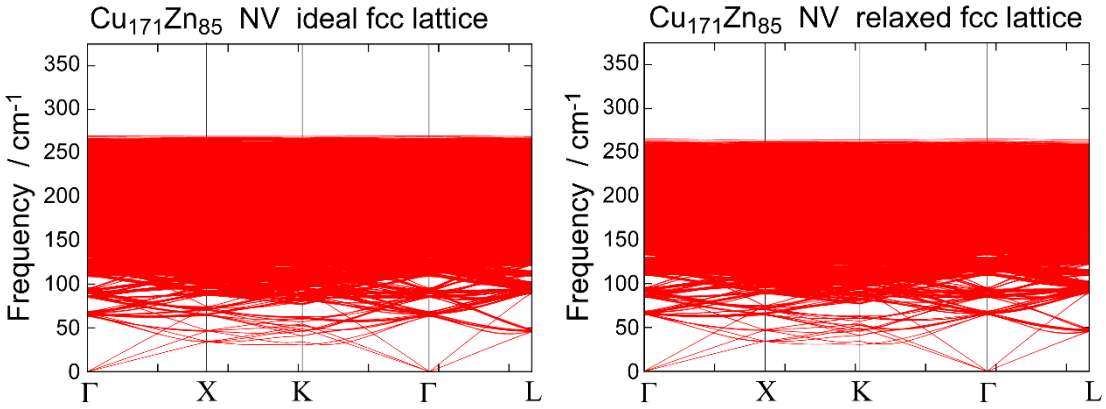

Fig. S6 Phonon dispersion obtained by the theoretical normal vibrational analysis of the $Cu_{171}Zn_{85}$ superlattices for the ideal *fcc* lattice and relaxed (structurally optimized) lattice, using the EAM potentials.

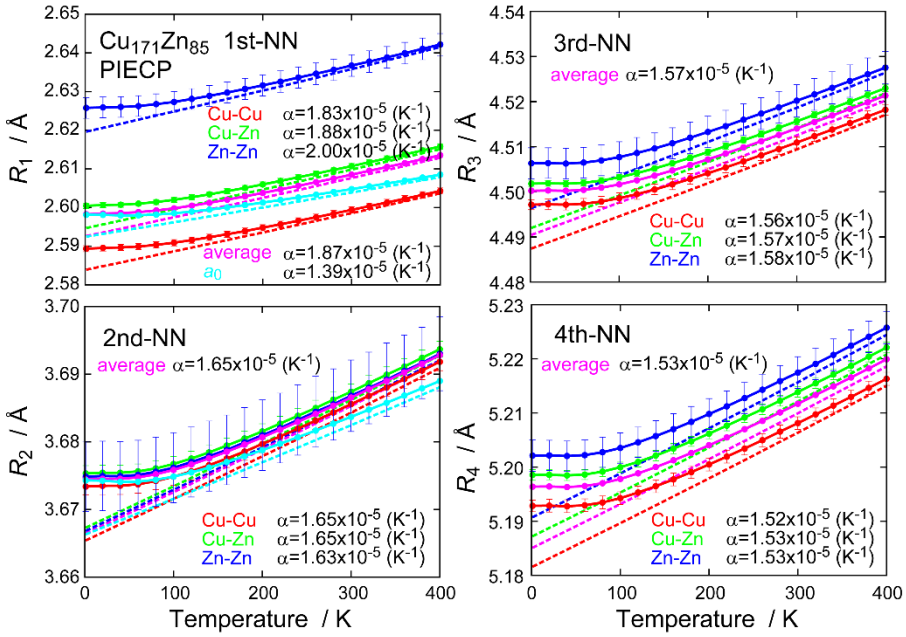

Fig. S7 Temperature dependence of the interatomic distances for the first- to fourth-NN shells in the PIECP simulations of $Cu_{171}Zn_{85}$. The estimated thermal expansion coefficient at ~300 K for each curve is given in the figure.

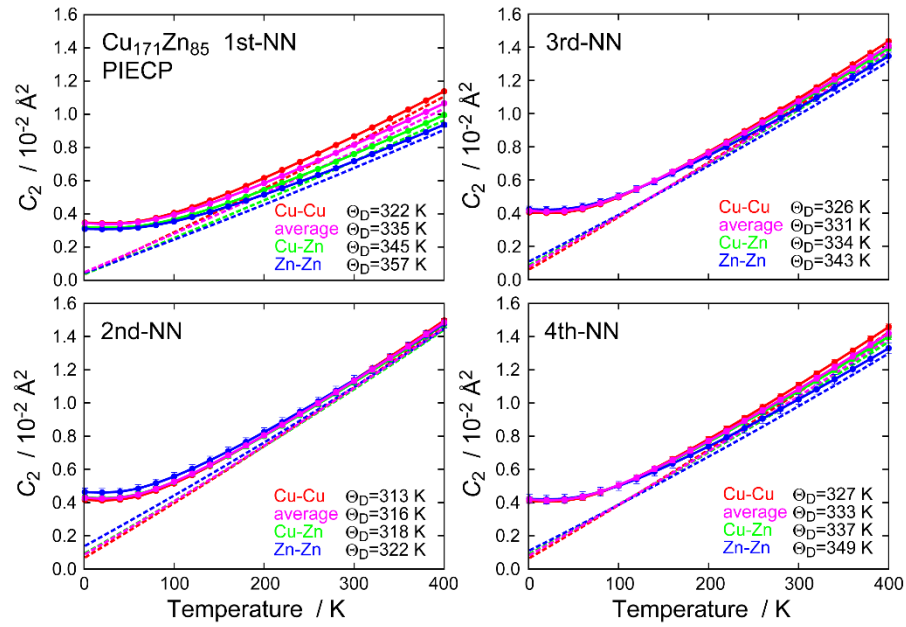

Fig. S8 Temperature dependence of the Debye-Waller factors C_2 for the first- to fourth-NN shells in the PIECP simulations of $Cu_{171}Zn_{85}$. The estimated Debye temperature for each curve is given in the figure.

Table S1 k and R ranges in the EXAFS analysis. Δk_{FT} is the Fourier transform k range, ΔR_{fit} the inverse Fourier transform R range, and Δk_{fit} is the curve-fitting k range. N_d is the independent data point given as $N_d \simeq 2\Delta k_{fit}\Delta R_{fit}/\pi + 1$.

First NN	Δk_{FT} (Å^{-1})	ΔR_{fit} (Å)	Δk_{fit} (Å^{-1})	N_d
Cu K edge	2.6-12.7	1.8-2.8	3.0-12.5	7.05
Zn K edge	2.4-15.7	1.7-2.7	3.0-15.5	8.96

Second to Fourth NN	Δk_{FT} (Å^{-1})	ΔR_{fit} (Å)	Δk_{fit} (Å^{-1})	N_d
Cu K edge	2.6-12.7	3.10-5.35	4.0-12.5	13.18
Zn K edge	2.4-15.7	3.10-5.30	5.0-14.0	13.61

Table S2 Results of the EXAFS analysis for the first-NN shells using the FEFF standards. The values in italic are the fixed parameters in the curve-fitting analysis. The values in the parentheses are the estimated 3σ errors.

Data	Method	shell	NS_0^2	R (Å)	ΔE_0 (eV)	C_2 (10^{-2} Å^2)	R-factor	χ^2	χ_ν^2
Cu K edge 21K	1-shell	average	11.09(12)	2.591(1)	0.2(2)	0.499(6)	0.0402	77.0	25.3
	2-shell	Cu-Cu	*7.17*	2.557(1)	-2.9(3)	0.701(14)	0.0339	54.6	52.1
		Cu-Zn	*3.91*	2.601(1)	-0.4(3)	0.181(10)			
Zn K edge 21K	1-shell	average	10.97(14)	2.603(1)	-2.7(2)	0.571(7)	0.0357	69.3	14.0
	2-shell	Zn-Cu	*7.10*	2.598(1)	-3.6(3)	0.655(13)	0.0369	73.8	25.0
		Zn-Zn	*3.87*	2.606(1)	-1.7(4)	0.458(14)			

The reliability factors are defined as

$$R\text{-factor} = \sqrt{\sum_{i=1}^{N_p}\left(\chi_{obs}(k_i) - \chi_{calc}(k_i)\right)^2 \Big/ \sum_{i=1}^{N_p}\left(\chi_{obs}(k_i)\right)^2}$$

for the R-factor, and χ^2 and χ_ν^2 are given as

$$\chi^2 = \frac{N_d}{N_p}\sum_{i=1}^{N_p}\left(\frac{\chi_{obs}(k_i) - \chi_{calc}(k_i)}{\varepsilon(k_i)}\right)^2 \quad \text{and} \quad \chi_\nu^2 = \frac{1}{N_d - N_{fit}}\frac{N_d}{N_p}\sum_{i=1}^{N_p}\left(\frac{\chi_{obs}(k_i) - \chi_{calc}(k_i)}{\varepsilon(k_i)}\right)^2,$$

where N_p and N_{fit} are the numbers of total data points and fitting variables, and $\varepsilon(k_i)$ the error at k_i.

Table S3 Results of the EXAFS analysis for the second- to fourth-NN shells using the FEFF standards. The values in the parentheses are the estimated 3σ errors.

Data	shell	NS_0^2	R (Å)	ΔE_0 (eV)	C_2 (Å^2)	R-factor	χ^2	χ_ν^2
Cu K edge 21K	2nd	14.3(9)	3.698(4)	3.3(5)	1.07(4)	0.0439	51.3	43.7
	3rd	24.0(7)	4.508(2)	-2.0(2)	0.61(2)			
	4th	15.5(5)	5.185(2)	-4.5(2)	0.76(2)			
Zn K edge 21K	2nd	12.2(11)	3.683(6)	-1.3(7)	1.18(6)	0.0353	40.4	25.2
	3rd	35.0(13)	4.492(2)	-7.4(3)	0.99(2)			
	4th	22.8(8)	5.209(2)	-4.0(2)	0.94(2)			

Table S4 EAM Potential parameters of *fcc* Cu, *hcp* Zn, L_{12} $CuZn_3$, and L_{12} Cu_3Zn to simulate the brass as $Cu_{171}Zn_{85}$. See for the definitions of the potential parameters, for instance, H. -S. Jang, D. Seol, and B. -J. Lee, *J. Magnes. Alloy* **9**, 317-335 (2021); DOI: 10.1016/j.jma.2020.09.006.

	E_c (eV)	r_e (Å)	B (GPa)	α	d
fcc Cu	3.54	2.543	142.0	5.1551	0.05
hcp Zn	1.09	2.638	70.4958	3.3423	0.05
L_{12} $CuZn_3$	1.70	2.614	88.4	6.0694	0.05
L_{12} Cu_3Zn	2.93	2.567	124.1	5.3366	0.05

	β_0	β_1	β_2	β_3	t_1	t_2	t_3	A
Cu	3.83	2.20	6.00	2.20	2.72	3.04	1.95	0.94
Zn	3.50	3.00	0.00	2.00	3.00	6.00	-10.0	0.70

	C_{min}	C_{max}
CuCuCu	1.21	2.80
ZnZnZn	1.00	2.80
CuZnCu	1.21	2.80
ZnCuZn	1.00	2.80
CuCuZn	1.1025	2.80
CuZnZn	1.1025	2.80